Role of mitochondrial-derived oxidants in renal tubular cell cold storage injury

Tanecia Mitchell[1,2], **Hamida Saba**[1,2], **Joe Laakman**[1], **Nirmala Parajuli**[1], and **Lee Ann MacMillan-Crow**[1]

[1]Department of Pharmacology and Toxicology, University of Arkansas for Medical Sciences, Little Rock, AR, USA

[2]Interdisciplinary Biomedical Sciences Graduate Program, University of Arkansas for Medical Sciences, Little Rock, AR, USA

Abstract

Cold storage (CS) is regarded as a necessary procedure during donation of a deceased donor kidney that helps to optimize organ viability. Increased oxidant generation during both CS as well as during the reperfusion (or rewarming/CS.RW) phase have been suggested to be a major contributor to renal injury; although the source and/or biochemical pathways involved with oxidant production remain unclear. The purpose of this study was to determine if renal tubular mitochondrial superoxide is capable of inducing oxidant production and mitochondrial damage in response to a CS.RW insult. To test the role of mitochondrial superoxide in CS.RW injury, we used rat renal proximal tubular (NRK) cells overexpressing manganese superoxide dismutase (MnSOD), the major mitochondrial antioxidant. Oxidant production, mitochondrial membrane potential, respiratory complex function, and cell death were all altered following exposure of NRK cells to CS.RW. MnSOD overexpression or inhibition of nitric oxide synthase (NOS) provided significant protection against oxidant generation, respiratory complex inactivation, and cell death. These findings implicate mitochondrial superoxide, nitric oxide, and their reaction product, peroxynitrite, as key signaling molecules involved in CS.RW injury of renal tubular cells, and suggest that therapeutic inhibition of these pathways may protect the donor kidney.

Keywords

Cold preservation; cold storage; superoxide; nitric oxide; peroxynitrite; mitochondria; respiratory complexes

INTRODUCTION

Cold storage (CS) is regarded as a critical step in the process of transplanting a deceased donor kidney, and is used to lower cellular metabolism, maintain organ viability and provide time for tissue matching between donor and recipient [1]. Despite its advantages and the design of preservation solutions to enhance organ viability, CS and the subsequent

Corresponding Author: Lee Ann MacMillan-Crow, Ph.D., Department of Pharmacology and Toxicology, University of Arkansas for Medical Sciences, 325 Jack Stephens Drive, Biomedical Building I, 323D, Little Rock, AR 72205, Tel.: 501-686-5289; Fax: 501-686-8970, lmcrow@uams.edu.

reperfusion phase that follows transplantation are associated with renal injury [2–4]. The injury caused by CS/reperfusion may partially explain why long-term renal function is compromised in kidneys harvested from deceased donors compared to kidneys transplanted from either living related or unrelated donors that avoid the cold preservation process [5–7].

'Static' CS consists of harvesting a kidney from a donor, flushing it with pre-cooled preservation solution, and then storing it in preservation solution at ~4°C until the transplantation surgery. The University of Wisconsin (UW)-Viaspan solution has become the standard CS solution for renal preservation, and its development by Belzer and Southard [8] has allowed deceased donor kidneys to be preserved for up to 72 hours [9–11], although most are transplanted by 24 hours [12–14]. Despite this advancement, several studies have revealed that donor kidneys exposed to CS for longer periods have more severe kidney injury following transplantation [14–16]. Unfortunately, the cellular mechanisms leading to CS/reperfusion injury are poorly understood, so rational strategies to minimize these detrimental outcomes are needed.

CS induced renal cell injury has been shown to be dependent on oxygen, because studies using hypoxic proximal tubular cells have documented less cellular damage compared to normoxic cells placed in CS [17,18]. These findings confirm the need to better understand the role that oxygen radicals play in CS mediated injury. Mitochondrial superoxide is a free radical that is thought to be continually generated by misfires (~1 to 2% of total oxygen consumption under non-physiological conditions) in the electron transport chain [19,20]. Superoxide can also be generated from other sources such as, its production by NADPH oxidase (or NOX) during the "respiratory burst" noted in activated phagocytes and from other cell types containing an isoform of NOX [21–25]. Superoxide is the proximal oxidant species involved in the formation of other oxidants including the hydroxyl radical, hydrogen peroxide, and peroxynitrite. Thus, it is strategically positioned to unleash several oxidant cascades associated with tissue injury. Manganese superoxide dismutase (MnSOD) is a nuclear encoded protein localized to the mitochondria where it dismutates mitochondrial superoxide to hydrogen peroxide within the mitochondrial matrix; hydrogen peroxide is then efficiently detoxified by catalase or glutathione peroxidase.

The goal of the present study was to elucidate the oxidant signaling pathway that is activated during CS.RW to trigger renal tubular cellular and mitochondrial injury. Our hypothesis was that mitochondrial superoxide contributes to oxidant production and mitochondrial damage during renal cell CS. We used an *in vitro* model of rat renal proximal tubular (NRK) cells to permit us to accurately monitor mitochondrial oxidant production using fluorescent imaging and also to have the capability to transiently transfect cells with MnSOD to lower available mitochondrial superoxide levels during CS.RW. Using this experimental strategy, our results provide initial evidence that mitochondrial superoxide is generated in NRK cells in response to CS, and the resulting oxidant production is associated with mitochondrial dysfunction and cell death.

MATERIALS AND METHODS

Cold Storage ± Rewarming Cell Model

Normal rat kidney proximal tubular cells (NRK-52E; American Type Culture Collection No. CRL-1571, USA) were maintained in either 6-well, 100mm, or 150mm size plates in a humidified incubator gassed with 5% CO_2, 95% air at 37°C in Dulbecco's Modified Eagle Medi um (DMEM) containing 5% fetal calf serum (FCS). Cells were grown to 60% confluency, and then divided into three treatment groups: (1) Untreated, (2) Cold Storage (CS), (3) Cold Storage and Rewarming (CS.RW). Untreated cells remained in DMEM containing 5% FCS for 24 h or 48 h at 37°C. CS (Groups 2 and 3) was initiated by washing

cells with cold PBS twice and storing them in University of Wisconsin/Viaspan (UW) solution for 24 h at 4°C. To simulate RW (Group 3), the UW solution was replaced after 24 h of CS with DMEM containing 5% FCS for 6 h at 37°C.

MnSOD Overexpression

NRK cells grown to 60% confluency were transiently transfected with the pMnSOD plasmid (10 µg) encoding the human MnSOD gene using lipofectamine (Invitrogen, USA) in OPTI-MEM (Invitrogen, USA) for 6 h at 37°C; non-transfected cells were incubated in OPTI-MEM alone [26,27]. After 6 h, all cells were treated with DMEM containing 5% FCS overnight at 37°C. The next day, cells were placed in one of the three treatment groups (Group 1, 2 or 3) mentioned above. MnSOD enzymatic activity was measured in cellular extracts using the cytochrome c reduction method [28] and was determined to have a 2-fold increase in activity compared to non-transfected cells (data not shown). In addition, transfection efficiency was determined to be 93% using a MnGFP plasmid containing the same vector used for MnSOD overexpression and green fluorescent protein (GFP) (data not shown). Efficiency was calculated as the ratio of the number of cells displaying green fluorescence by the total number of cells in a field times 100 (field size: 40X).

Mitochondrial Superoxide Production

MitoSOX Red (Molecular Probes, USA) was used to detect mitochondrial superoxide production in Groups 1, 2, and 3. This modified cationic dihydroethidium dye is localized to the mitochondria where it is oxidized by superoxide to generate a bright red fluorescence [29]. Briefly, cells were preloaded in the dark with MitoSOX red (5 µM for 10 min) prior to treatment. Fluorescence was visualized using a Nikon Eclipse E800 microscope with a rhodamine filter using a water immersion objective (60X). All images were captured with equal exposure times. Fluorescent images were quantified for each sample by averaging the mean intensity fluorescence of 5 random cells in three different fields using Nikon Nis Elements software. Additionally, cells were grown on coverslips, preloaded with MitoSOX Red prior to treatment (Group 1, 2 or 3) and evaluated for mitochondrial superoxide generation using a Hitachi spectrofluorometer equipped with a coverslip holder using 2 different excitation wavelengths: 396 nm and 510 nm with the emission measured at 580 nm as previously described [27,29].

Nitric Oxide Measurement

Available nitric oxide levels were determined for all three groups by loading NRK cells with Diaminorhodamine 4M-AM (DAR, 5µM; Calbiochem, USA) 30 minutes prior to the end of treatment in the dark. DAR is a non-fluorescent compound that in the presence of nitric oxide and oxygen forms a fluorescent triazolo-rhodamine analog [30]. Fluorescence was evaluated using a Nikon Eclipse E800 microscope with a rhodamine filter using a water immersion objective (60X). All images were captured with equal exposure times. Fluorescent images were quantified for each sample by averaging the mean intensity fluorescence of 5 random cells in three different fields using Nikon Nis Elements software.

Nitrotyrosine Immunocytochemistry

NRK cells from Groups 1, 2 and 3 were washed with cold PBS, fixed for 15 min with 4% Formalin, washed with PBS and permeabilized with 0.1% Triton X-100/0.1% Sodium citrate for 2 min on ice. Cells were then washed with PBS and blocked with 3% bovine serum albumin (Sigma-Aldrich, USA) in PBS for 1 h, followed by overnight incubation at 4°C with the rabbit polyclonal nitrotyrosine antibody (1:200; Millipore, USA). The following day, cells were washed with PBS-Tween (0.1%), PBS, and incubated with the goat anti-rabbit IgG Alexa-594 antibody (1:1000; Invitrogen, USA) for 30 min in the dark at

room temperature (RT). Cells were rinsed with PBS-Tween (0.1%), and nuclear counterstaining was initiated using DAPI (1:100; Invitrogen, USA) for 10 min at RT. Subsequently, cells were washed and coverslipped with ProLong Gold Anti-fade Reagent with DAPI (Invitrogen, USA). Nitrotyrosine staining was evaluated with a Nikon Eclipse 800 microscope (40X Oil). All images were captured with equal exposure times. NRK cells treated with peroxynitrite (0.8mM) in PBS for 5 min at RT served as positive controls. The negative controls were NRK cells treated with peroxynitrite but the nitrotyrosine antibody was pre-incubated with excess 3-nitrotyrosine (10 mM; Sigma-Aldrich, USA) prior to adding to permeabilized cells. In separate experiments, cells were pre-treated with the following inhibitors at 37°C to evaluate the role of specific oxidants during CS: Diphenyleneiodonium chloride (DPI, 1μM for 1h; Sigma-Aldrich, USA) to inhibit NADPH oxidase, Catalase (2000 Units/mL for 30 min; Sigma-Aldrich, USA) to block hydrogen peroxide, and N5-[imino(methylamino)methyl]-L-ornithine, citrate (L-NMMA, 100μM for 30 min; Cayman, USA) to inhibit nitric oxide synthases (NOS); inhibitors were also included for the duration of CS exposure.

Mitochondrial Membrane Potential Assessment

The relative mitochondrial membrane potential was determined using a lipophilic cationic probe 5, 5′, 6, 6′-tetrachloro-1,1′,3,3′-tetraethylbenzimdazol-carbocyanine iodide (JC-1; Molecular Probes, USA). All treatment groups were incubated in the dark with JC-1 (7.5 μM for 30 min). Fluorescence was observed using a Nikon Eclipse 800 microscope with a 60X water immersion objective equipped with a dual filter for fluorescein and rhodamine. Green staining is indicative of the monomeric form of JC-1 (i.e. lower membrane potential) and the red staining corresponds to the aggregate form (i.e. higher membrane potential). Thus, yellow staining indicates relatively normal membrane potential (combined aggregate and monomer). Average mean intensity fluorescence was calculated using the ratio of JC-1 aggregate/monomer (590 nm/530 nm) using the Nikon Nis Elements software. All images were captured with equal exposure times.

Measurement of Respiratory Complexes Activity

NRK cell mitochondria were isolated by centrifugation on a sucrose density gradient, and the activity of mitochondrial Complexes I thru IV were assayed spectrophotometrically at 30°C [31]. Complex I (NADH: Ubiquinone Oxidoreductase) activity was measured by the oxidation of NADH (Sigma-Aldrich, USA) at 340 nm. Complex II (Succinate: Ubiquinone Oxidoreductase) activity was determined by the reduction of dichlorophenolindophenol (Sigma-Aldrich, USA) at 595 nm. Complex III (Ubiquinol: Cytochrome c Oxidoreductase) activity was evaluated by the reduction of cytochrome c (III) (Sigma-Aldrich, USA) at 550 nm. Complex IV (Cytochrome c Oxidase) activity was assessed by following oxidation of reduced cytochrome c (II) (Sigma-Aldrich, USA) at 550 nm. The changes in absorbance in blank samples (containing no mitochondria) were recorded for all assays.

Cell Cytotoxicity Assessment

NRK cytotoxicity was determined using the LDH-Cytotoxicity Assay Kit II (Biovision Research Products, USA). This kit uses water soluble tetrazolium salt (WST) reagent to react with NADH produced by lactate from lactate dehydrogenase (LDH), to give an intense yellow color directly correlating with the amount of LDH in the media. Absorbance was measured at 450 nm using a SpectraMax 190 microplate reader using SpectraMax software (Molecular Devices, USA).

Statistical Analysis

Results are presented as mean ± standard error of the mean (SEM). Means were obtained from at least three independent experiments. One way analysis of variance (ANOVA) was used to compare the mean values among the untreated and treatment groups, followed by Tukey's test to compare differences in mean between two groups at 95% level of confidence using the Origin 6.0 statistical software. Differences with a P value less than 0.05 was considered statistically significant.

RESULTS AND DISCUSSION

MnSOD overexpression decreases measurable superoxide during CS and RW of renal tubular cells

Since superoxide plays a central role in oxidant generation, we initially evaluated the role of mitochondrial superoxide in a cell model of CS-induced injury and rewarming (RW) in which proximal tubular NRK cells were exposed to 24 h of CS with or without 6 h of RW. For the current studies, we used MitoSOX Red, a dye that is directly targeted to the mitochondria to detect available mitochondrial superoxide. Using this strategy, we observed that 24 h of CS significantly increased the MitoSOX Red signal associated with mitochondrial superoxide compared to untreated (Untx) control cells (CS alone 885.7 ± 47.1 vs. Untx 68.4 ± 15.1 mean fluorescence intensity) (Figure 1A, B). However, available mitochondrial superoxide levels decreased significantly following 6 hr RW (CS.RW 130.2 ± 6.9 mean fluorescence intensity) (Figure 1A, B).

MitoSOX Red can yield two distinct fluorescent species upon oxidation by superoxide: mito-hydroxyethidium and mito-ethidium, and their fluorescence emission at 580 nm can be selectively measured by using distinct excitation wavelengths, 396 nm and 510 nm respectively [29]. Fluorescence microscopy cannot discriminate between these species, however a spectrofluorometric based assay using cells grown on coverslips can be used to distinguish between the two distinct MitoSOX Red fluorescent species [27]. NRK cells exposed to CS showed a significant increase in MitoSOX red fluorescence at the 396 nm excitation wavelength (mito-hydroxyethidium) (CS 2.2 ± 0.1 vs. Untx 1.0 ± 0 mean fold change in arbitrary fluorescence value) (Figure 1C), but no increase in MitoSOX Red staining was observed using the 510 nm excitation wavelength (mito-ethidium) (CS 1.1 ± 0.1 vs. Untx 1.0 ± 0 mean fold change in arbitrary fluorescence value) (Figure 1D). Consistent with the fluorescence microscopy results, MitoSOX Red staining was decreased following RW (15 min or 6 h) (CS.RW (15 min) 1.2 ± 0.2 vs. CS.RW (6 h) 1.1 ± 0.1 vs. Untx 1.0 ± 0 mean fold change in arbitrary fluorescence value) (Figure 1C).

These observations extended an earlier finding by Salahudeen *et al.* [32] that demonstrated superoxide is generated by human proximal tubular cells during 24 h of CS. However, the cytochrome c reduction method used in this study failed to delineate the origin of superoxide generation, which we now hypothesize is from the mitochondria. The reduction in measurable superoxide during RW presumably reflects superoxide interacting with other oxidants and/or less mitochondrial generation of superoxide at the time of measurement. In order to verify that the changes in superoxide observed in NRK cells during CS and RW originated in the mitochondria, cells were transiently transfected with MnSOD, the major mitochondrial antioxidant responsible for scavenging superoxide. The CS-induced elevation of superoxide in MnSOD overexpressing cells was ~50% less than in non-transfected cells (450.7 ± 31.3 CS+MnSOD vs. CS alone 885.7 ± 47.1 mean fluorescence intensity) (Figure 1B). However, MnSOD overexpression did not affect superoxide levels during RW which were already restored to basal levels from the CS-induced peak (141.8 ± 11.7 CS.RW +MnSOD vs. CS.RW 130.2 ± 6.9 mean fluorescence intensity) (Figure 1A, B). As mentioned previously, superoxide can also be generated by non-mitochondrial sources

including NADPH oxidases [33]. We evaluated this possibility by treating NRK cells with diphenyleneiodonium chloride (DPI, 1 μM), a non-selective NADPH oxidase inhibitor for 1 h prior to and during CS. DPI treatment did not affect the rise in MitoSOX Red signal in response to 24 h of CS (data not shown), suggesting that NADPH oxidase was not involved in superoxide production during CS. These results support our hypothesis that mitochondrial superoxide is increased during CS of renal tubular cells.

Modulation of Nitric Oxide levels during CS and RW

Nitric oxide is a diffusible, free radical molecule that has many roles in physiology and pathophysiology. It can be synthesized by at least three forms of nitric oxide synthases (NOS) [34,35]. Nitric oxide and superoxide can react to form the powerful oxidant and nitrating agent peroxynitrite [36], hence we hypothesized that the increased superoxide produced during CS might lead to decreased nitric oxide levels. Thus, we evaluated available nitric oxide levels in NRK cells following CS and RW using diaminorhodamine 4M-AM (DAR). Nitric oxide levels in NRK cells exposed to 24 h of CS were significantly lower compared to untreated cells (CS 70.9 ± 20.4 vs. Untx 450.0 ± 27.0 mean fluorescence intensity) (Figure 2A, B). Subsequent rewarming (CS.RW) partially restored nitric oxide levels toward control values (CS.RW 326.0 ± 10.7 vs. Untx 450.0 ± 27.0 mean fluorescence intensity) (Figure 2A, B).

Overexpression of MnSOD did not significantly alter the CS-mediated loss in available nitric oxide levels. However, we unexpectedly observed that NRK cells overexpressing MnSOD had lower basal nitric oxide levels compared to non-transfected cells (MnSOD 319.8 ± 35.4 vs. Untx 450.0 ± 27.0 mean fluorescence intensity) (Figure 2A, B). These findings contradict the traditional view that scavenging superoxide (MnSOD overexpression) should increase the amount of available nitric oxide by minimizing nitric oxide-superoxide interaction that results in the formation of peroxynitrite. However, a recent study characterizing the chemical interaction between nitric oxide and pure MnSOD (from *E. coli*) by Filipovi et al. [37], suggest that MnSOD can actually catalyze the decay of nitric oxide under anaerobic and aerobic conditions. The study also showed that reaction of MnSOD with nitric oxide also resulted in partial inactivation of MnSOD. These authors speculate that MnSOD-mediated degradation of nitric oxide is a protective mechanism to defend against nitric oxide toxicities. It is important to point out that the studies described above were test tube studies, not performed in cells, thus it remains unknown whether these mechanisms can occur *in vitro* or *in vivo*. In our study, the mechanism(s) mediating the loss of nitric oxide in MnSOD-overexpressing cells are unknown, but we believe this intriguing finding warrants further experiments since it may reveal a new paradigm for MnSOD-nitric oxide interaction in renal tubular cells. The decline in nitric oxide levels observed in NRK cells exposed to CS, which occurred in the presence or absence of MnSOD transfection, could be due to cold temperatures inhibiting NOS activity or alternatively, that the available nitric oxide could be consumed by increased superoxide production thereby forming peroxynitrite.

Nitrotyrosine formation occurs during CS and RW of renal tubular cells and is decreased with MnSOD overexpression or NOS inhibition

Protein bound nitrotyrosine formation is a "footprint" widely used immunologically to demonstrate nitric oxide dependent oxidative damage (e.g. peroxynitrite formation). In this study, we used a polyclonal antibody against nitrotyrosine and a secondary antibody conjugated with goat anti-rabbit Alexa-594 to detect nitrotyrosine using immunocytochemistry. Since our earlier findings demonstrated both an increase in superoxide and a decrease in nitric oxide during CS, we then expected to see increased peroxynitrite (nitrotyrosine staining). As hypothesized, exposure of NRK cells to 24 h of CS

alone or with 6 hr of rewarming (CS.RW) resulted in increased nitrotyrosine formation (red staining) compared to untreated cells (Figure 3). MnSOD overexpression decreased nitrotyrosine formation during CS, suggesting less oxidant damage in the presence of enhanced superoxide scavenging. But surprisingly, a difference in nitrotyrosine staining was not readily apparent between non-transfected and MnSOD overexpressing NRK cells after CS.RW (Figure 3). The lack of significant protection by MnSOD during RW could reflect partial inactivation of MnSOD by peroxynitrite formation during CS.RW or that RW leads to nitration of non-mitochondrial targets that are inaccessible to MnSOD scavenging. Cells overexpressing MnSOD alone showed some background nitrotyrosine staining. Further control experiments using the secondary Alexa-594 antibody alone (MnSOD 2′ alone) revealed that this background staining was likely due to non-specific effects of the secondary antibody used in these studies (Figure 3). In addition, NRK cells treated with lipofectamine alone did not increase nitrotyrosine formation (data not shown).

To provide stronger evidence that peroxynitrite is the oxidant likely involved with tyrosine nitration during CS, we used the non-selective NOS inhibitor, N5-[imino(methylamino)methyl]-L-ornithine, citrate (L-NMMA, 100 μM for 30 min prior to and during CS), to block nitric oxide synthesis. Similar to the effect of MnSOD overexpression, nitric oxide blockade prevented the increased tyrosine nitration seen during CS (Figure 3). To determine whether NOX might contribute to tyrosine nitration (the superoxide component), NRK cells were treated with the NOX inhibitor, DPI (1 μM for 1 h prior to and during CS). DPI treatment did not decrease NRK cell nitrotyrosine formation during CS (Figure 3). Finally, hydrogen peroxide also appeared to have no role in CS induced tyrosine nitration since catalase treatment (2000 Units/mL for 30 min prior to and during CS) did not alter nitrotyrosine staining (Figure 3). The Amplex Red Assay was also performed and showed no increase in hydrogen peroxide levels following CS of NRK cells (data not shown). These findings strongly suggest that peroxynitrite is the primary oxidant leading to nitrotyrosine formation during CS of renal tubular cells.

MnSOD overexpression doesn't protect against CS induced mitochondrial membrane depolarization

A few studies have documented mitochondrial abnormalities induced by CS, including: mitochondrial swelling, loss of ATP, and mitochondrial dependent apoptosis with RW [38,39]. However, the 'triggers' or signaling pathways that lead to such mitochondrial damage have not been explored in depth. Thus, we sought to determine whether increases in mitochondrial superoxide lead to altered mitochondrial function during CS. One way to assess mitochondrial function is to measure the relative mitochondrial membrane potential, generated by oxidative phosphorylation, using the cationic probe JC-1. NRK cells exposed to CS alone had significantly lower (depolarized) relative mitochondrial membrane potential (green staining) when compared to untreated cells, which were depicted by normal red/green/yellow staining (Figure 4A). The mitochondrial depolarization observed following CS of NRK cells is consistent with other reports showing early mitochondrial structural abnormalities during CS using electron microscopy [38]. Cold temperatures can lead to a rapid decline in ATP levels [40,41] suggesting that cold slows down oxidative phosphorylation drastically. This slowing of oxidative phosphorylation could explain why depolarization of mitochondria occurred during CS of NRK cells. Lipofectamine treatment of NRK cells did not alter mitochondrial membrane potential (data not shown). Mitochondrial membrane potential was restored to basal levels following RW of NRK cells (CS.RW 1.24 ±.07 vs. Untx 1.28 ±.06 mean fluorescence intensity) (Figure 4A, B). The reason for this restoration of mitochondrial membrane potential is unknown; however, it could be in response to the cells returning to their normal physiological state (37°C) or that depolarization was a transient event. Hence, it is possible that during the CS-induced

depolarization, superoxide is generated which leads to further injury during RW even though the mitochondrial membrane potential has returned to basal levels during RW.

Overexpression of MnSOD in NRK cells did not significantly alter mitochondrial depolarization during CS (CS+MnSOD 0.18 ±.09 vs. CS 0.13 ±.07 mean fluorescence intensity) (Figure 4A, B). This suggests that mitochondrial depolarization during CS may not be a result of mitochondrial superoxide, or downstream oxidant production, but rather an effect of the lowered temperature. However, it remains possible that the CS-induced mitochondrial depolarization may be responsible, in part, for the increased levels of mitochondrial superoxide observed in NRK cells during CS.

MnSOD overexpression or NOS inhibition protects against partial inactivation of mitochondrial respiratory complexes during CS

Disruption of mitochondrial respiratory complexes can lead to generation of oxidants, mitochondrial depolarization, and cell injury [42–44]. We have previously documented that the activity of all four mitochondrial respiratory complexes were declined using an *in vivo* cold I/R model (40 minutes of cold ischemia followed by 18 h of reperfusion) [45]. Thus, experiments were carried out to determine whether CS alone or with RW alters NRK cell mitochondrial respiratory complex activity. Complexes I and II were significantly inactivated following 24 h of CS alone when compared to untreated NRK cells (Complex I: CS 58.3 ± 4.0 vs. 100 % of control; Complex II: CS 53.1 ± 1.7 vs. 100 % of control) (Figure 5A, B). NRK cells exposed to CS.RW showed a significant decline in activity of respiratory Complexes I, II, and III when compared to untreated cells (Complex I: CS.RW 43.1 ± 3.8 vs. 100 % of control; Complex II: CS.RW 41.5 ± 4.8 vs. 100 % of control; Complex III: CS.RW 54.4 ± 6.3 vs. 100 % of control) (Figure 5A–C). Additional experiments measuring mitochondrial oxygen consumption/respiration during CS were attempted but, NRK cells were not efficient in responding to traditional oxygen consumption substrates which may be due to NRK cells' heavy reliance on glycolytic pathways.

Overexpression of MnSOD in NRK cells prevented inactivation of Complexes I and II during CS (Complex I: CS+MnSOD 80.2 ± 9.8 vs. CS 40.0 ± 3.8; Complex II: CS+MnSOD 97.3 ± 4.4 vs. CS $41.5 \pm 9.1\%$) (Figure 5E, F). This finding suggests that increased mitochondrial superoxide contributes to the partial inactivation of Complex I and II observed during CS. In addition, the contribution of nitric oxide on respiratory complex inactivation during CS was evaluated using the non-selective NOS inhibitor, L-NMMA. L-NMMA treatment prior to and during CS also provided protection against respiratory complex inactivation of Complexes I and II during CS (Complex I: CS+L-NMMA 91.9 ± 8.7 vs. CS 40.0 ± 3.8; Complex II: CS+L-NMMA 97.0 ± 11.2 vs. CS $41.5 \pm 9.1\%$) (Figure 5E, F). These data demonstrate that both mitochondrial superoxide and nitric oxide (strongly supporting a role for peroxynitrite) contribute to CS-mediated damage to mitochondrial respiratory complexes during CS, which is in agreement with previous studies in other systems [46–48].

Several studies have suggested that respiratory Complexes I and III serve as the major sources for generation of superoxide in the mitochondria [49,50]. Conversely, respiratory Complexes I and III have also been reported as a target for oxidative damage by reactive oxygen species [48,51]. Thus, it appears that mitochondrial complexes could serve as a source or a target for reactive oxygen species, depending upon the mechanisms governing the etiology of a disease.

MnSOD overexpression or NOS inhibition protects against cell death during CS and RW of renal tubular cells

Previous studies have documented that CS.RW of renal proximal tubular cells leads to cell death [32,38,39]. Salahudeen et al. showed that the mode of cell death was primarily apoptotic when cells were exposed to CS.RW; however, CS resulted in minimal cell death [38]. Consistent with these findings, NRK cells exposed to CS showed no significant increase in cell death, but was significantly increased following RW (Untx 6.1 ± 2.3 % vs. CS 9.4 ± 0.6 % vs. CS.RW 38.1 ± 3.9%) (Figure 6). NRK cells overexpressing MnSOD provided partial protection against cell death during CS.RW (CS.RW+MnSOD 25.8 ± 1.3% vs. CS.RW 38.1 ± 3.9%) (Figure 6), which revealed that mitochondrial superoxide contributes to cell death during CS.RW. Further studies were performed to evaluate the role of nitric oxide in cell death induced by CS.RW using the non-selective NOS inhibitor, L-NMMA. NRK cells treated with L-NMMA alone resulted in a slight, but not significant increase in cell death when compared to untreated cells (L-NMMA 11.3 ± 1.9 % vs. Untx 6.1 ± 2.3 %) (Figure 6). Interestingly, NRK cells treated with L-NMMA (30 minutes prior to and during CS) blunted cell death significantly during CS.RW, implicating that nitric oxide plays a pivotal role in cell death during CS.RW (CS.RW+L-NMMA 13.6 ± 2.9% vs. CS.RW 38.1 ± 3.9%) (Figure 6). These data support the possibility that peroxynitrite is produced during CS and RW and leads to NRK cell death (Figure 7).

It is known that respiratory complexes can 'leak' superoxide to the matrix side of the mitochondria or towards the cytosol/intermembrane space-a location that would preclude protection by the matrix localized antioxidant, MnSOD [52,53]. This may provide further insight into the data showing that MnSOD overexpression provided a modest, but significant protection from cell death following CS.RW; while pretreatment with L-NMMA provided a more robust protection. Hence, it is possible that CS.RW causes superoxide flux towards the cytosol, generating peroxynitrite and tyrosine nitration of non-mitochondrial matrix targets which lead to cell death. This hypothesis is actually supported by our nitrotyrosine staining shown in Figure 3, where overexpression of MnSOD failed to lower nitrotyrosine staining during CS.RW.

Many other studies have implicated 'reactive oxygen species' in CS-induced damage by using generic oxidant scavengers or non-specific assays for oxidant detection [32,33,39,54,55]; our current results represent the first known assessment of the extent and identity of oxidant production and mitochondrial dysfunction in renal tubular cells following CS alone and with RW. The data presented here provide support for the idea that blocking superoxide generation during CS might lead to prevention of numerous downstream pathways known to elicit renal injury during cold preservation/reperfusion prior to transplantation (Figure 7).

Future studies are underway to address the benefit of adding mitochondrial superoxide or more broad-spectrum oxidant scavengers to preservation solutions to mitigate injury during CS.RW. Application of these findings could provide healthier donor kidneys, offer improved graft function, and enhanced quality of life for graft recipients. The data presented in this study can be used later to validate animal models or could be applicable in testing compounds specifically designed to protect against CS-mediated cellular injury.

Acknowledgments

ABBREVIATIONS

|	
CS	Cold Storage
CS.RW	Cold Storage+Rewarming
DAR	Diaminorhodamine-4M AM
DPI	Diphenyleneiodonium chloride
I/R	Ischemia/Reperfusion
JC-1	5, 5′, 6, 6′-tetrachloro-1,1′,3,3′-tetraethylbenzimdazol-carbocyanine iodide
LDH	Lactate dehydrogenase
L-NMMA	N5-[imino(methylamino)methyl]-L-ornithine, citrate
MnSOD	Manganese Superoxide Dismutase
$^{\bullet}$NO	Nitric Oxide
NOS	Nitric Oxide Synthase
NOX	NADPH Oxidase
NRK	Normal Rat Kidney Proximal Tubular Cells
$O_2^{\bullet-}$	Superoxide
$ONOO^{-}$	Peroxynitrite
RW	Rewarming
UW	University of Wisconsin/Viaspan Solution

References

1. Salahudeen AK. Cold ischemic injury of transplanted kidneys: new insights from experimental studies. Am J Physiol Renal Physiol. 2004; 287:F181–F187. [PubMed: 15271685]

2. Henke W, Jung K, Polster F. Effects of preservation solutions on cortical and medullary mitochondria of rat kidney. Cell Mol Biol (Noisy -le-grand). 1995; 41:319–326. [PubMed: 7787743]

3. Sammut IA, Burton K, Balogun E, Sarathchandra P, Brooks KJ, Bates TE, Green CJ. Time-dependent impairment of mitochondrial function after storage and transplantation of rabbit kidneys. Transplantation. 2000; 69:1265–1275. [PubMed: 10798740]

4. Wilson DR, Arnold PE, Burke TJ, Schrier RW. Mitochondrial calcium accumulation and respiration in ischemic acute renal failure in the rat. Kidney Int. 1984; 25:519–526. [PubMed: 6737843]

5. Knoll G. Trends in kidney transplantation over the past decade. Drugs. 2008; 68:3–10. [PubMed: 18442296]

6. Park YH, Min SK, Lee JN, Lee HH, Jung WK, Lee JS, Lee JH, Lee YD. Comparison of survival probabilities for living-unrelated versus cadaveric renal transplant recipients. Transplantation Proceedings. 2004; 36:2020–2022. [PubMed: 15518731]

7. 2008 Annual Report of the US Organ Procurement and Transplantation Network and the Scientific Registry of Tranpslant Recipients: Transplant Data 1998–2007. U.S. Department of Health and Human Services, Health Resources and Services Administration, Healthcare Systems Bureau, Division of Transplantation; Rockville, MD: 2008.

8. Southard JH, Belzer FO. Organ Preservation. Annual Review of Medicine. 1995; 46:235–247.

9. Southard JH, Senzig KA, Belzer FO. Effects of hypothermia on canine kidney mitochondria. Cryobiology. 1980; 17:148–153. [PubMed: 7398356]

10. Southard JH, Van der Laan NC, Lutz M, Pavlock GS, Belzer JP, Belzer FO. Comparison of the effect of temperature on kidney cortex mitochondria from rabbit, dog, pig, and human: Arrhenius plots of ADP-stimulated respiration. Cryobiology. 1983; 20:395–400. [PubMed: 6617229]

11. Southard JH, Lutz MF, Ametani MS, Belzer FO. Stimulation of ATP synthesis in hypothermically perfused dog kidneys by adenosine and PO4. Cryobiology. 1984; 21:13–19. [PubMed: 6609048]

12. Southard JH, Lindell SL, Belzer FO. Energy metabolism and renal ischemia. Ren Fail. 1992; 14:251–255. [PubMed: 1509157]

13. Salahudeen AK, May W. Reduction in cold ischemia time of renal allografts in the United States over the last decade. Transplant Proc. 2008; 40:1285–1289. [PubMed: 18589088]

14. Salahudeen AK, Haider N, May W. Cold ischemia and the reduced long-term survival of cadaveric renal allografts. Kidney Int. 2004; 65:713–718. [PubMed: 14717946]

15. Ojo AO, Wolfe RA, Held PJ, Port FK, Schmouder RL. Delayed graft function: risk factors and implications for renal allograft survival. Transplantation. 1997; 63:968–974. [PubMed: 9112349]

16. Shoskes DA, Cecka JM. Deleterious effects of delayed graft function in cadaveric renal transplant recipients independent of acute rejection. Transplantation. 1998; 66:1697–1701. [PubMed: 9884262]

17. Peters SM, Rauen U, Tijsen MJ, Bindels RJ, van Os CH, de Groot H, Wetzels JF. Cold preservation of isolated rabbit proximal tubules induces radical-mediated cell injury. Transplantation. 1998; 65:625–632. [PubMed: 9521195]

18. Bartels-Stringer M, Verpalen JT, Wetzels JF, Russel FG, Kramers C. Iron chelation or anti-oxidants prevent renal cell damage in the rewarming phase after normoxic, but not hypoxic cold incubation. Cryobiology. 2007; 54:258–264. [PubMed: 17391662]

19. Chance B, Sies H, Boveris A. Hydroperoxide Metabolism in Mammalian Organs. Physiological Reviews. 1979; 59:527–605. [PubMed: 37532]

20. Cochme H, Murphy MP. Mitochondria as a source of reactive oxygen species. Biochemical Journal Classic Papers. 2009

21. Griendling KK, Minieri CA, Ollerenshaw JD, Alexander RW. Angiotensin II stimulates NADH and NADPH oxidase activity in cultured vascular smooth muscle cells. Circ Res. 1994; 74:1141–1148. [PubMed: 8187280]

22. Mohazzabh KM, Wolin MS. Sites of Superoxide Anion Production Detected by Lucigenin in Calf Pulmonary-Artery Smooth-Muscle. American Journal of Physiology-Lung Cellular and Molecular Physiology. 1994; 11:L815–L822.

23. Pagano PJ, Ito Y, Tornheim K, Gallop PM, Tauber AI, Cohen RA. An NADPH oxidase superoxide-generating system in the rabbit aorta. Am J Physiol. 1995; 268:H2274–H2280. [PubMed: 7611477]

24. Shiose A, Kuroda J, Tsuruya K, Hirai M, Hirakata H, Naito S, Hattori M, Sakaki Y, Sumimoto H. A novel superoxide-producing NAD(P)H oxidase in kidney. Journal of Biological Chemistry. 2001; 276:1417–1423. [PubMed: 11032835]

25. Zulueta JJ, Yu FS, Hertig IA, Thannickal VJ, Hassoun PM. Release of hydrogen peroxide in response to hypoxia-reoxygenation: role of NAD(P)H oxidase-like enzyme in endothelial cell plasma membrane. Am J Resp Cell Mol Biol. 1995; 12:41–49.

26. Cruthirds DL, Saba H, MacMillan-Crow LA. Overexpression of manganese superoxide dismutase protects against ATP depletion-mediated cell death of proximal tubule cells. Arch Biochem Biophys. 2005; 437:96–105. [PubMed: 15820221]

27. Munusamy S, MacMillan-Crow LA. Mitochondrial superoxide plays a crucial role in the development of mitochondrial dysfunction during high glucose exposure in rat renal proximal tubular cells. Free Radical Biology and Medicine. 2009; 46:1149–1157. [PubMed: 19439219]

28. McCord JM, Fridovich I. Superoxide dismutase An enzymic function for erythrocuprein (hemocuprein). Journal of Biological Chemistry. 1969; 244:6049–6055. [PubMed: 5389100]

29. Robinson KM, Janes MS, Pehar M, Monette JS, Ross MF, Hagen TM, Murphy MP, Beckman JS. Selective fluorescent imaging of superoxide in vivo using ethidium-based probes. Proceedings of the National Academy of Sciences of the United States of America. 2006; 103:15038–15043. [PubMed: 17015830]

30. Kojima H, Hirotani M, Nakatsubo N, Kikuchi K, Urano Y, Higuchi T, Hirata Y, Nagano T. Bioimaging of nitric oxide with fluorescent indicators based on the rhodamine chromophore. Analytical Chemistry. 2001; 73:1967–1973. [PubMed: 11354477]

31. Birch-Machin MA, Turnbull DM. Assaying mitochondrial respiratory complex activity in mitochondria isolated from human cells and tissues. Methods Cell Biol. 2001; 65:97–117. [PubMed: 11381612]

32. Salahudeen AK, Huang H, Patel P, Jenkins JK. Mechanism and prevention of cold storage-induced human renal tubular cell injury. Transplantation. 2000; 70:1424–1431. [PubMed: 11118084]

33. Karhumaki P, Tiitinen SL, Turpeinen H, Parkkinen J. Inhibition of ERK 1/2 activation by phenolic antioxidants protects kidney tubular cells during cold storage. Transplantation. 2007; 83:948–953. [PubMed: 17460567]

34. Knowles RG, Moncada S. Nitric-Oxide Synthases in Mammals. Biochemical Journal. 1994; 298:249–258. [PubMed: 7510950]

35. Brown GC, Borutaite V. Nitric oxide, mitochondria, and cell death. Iubmb Life. 2001; 52:189–195. [PubMed: 11798032]

36. Padmaja S, Huie RE. The reaction of nitric oxide with organic peroxyl radicals. Biochemical & Biophysical Research Communications. 1993; 195:539–544. [PubMed: 8373394]

37. Filipovic MR, Stanic D, Raicevic S, Spasic M, Niketic V. Consequences of MnSOD interactions with nitric oxide: Nitric oxide dismutation and the generation of peroxynitrite and hydrogen peroxide. Free Radical Research. 2007; 41:62–72. [PubMed: 17164179]

38. Salahudeen AK, Huang H, Joshi M, Moore NA, Jenkins JK. Involvement of the mitochondrial pathway in cold storage and rewarming-associated apoptosis of human renal proximal tubular cells. Am J Transplant. 2003; 3:273–280. [PubMed: 12614281]

39. Bartels-Stringer M, Kramers C, Wetzels JF, Russel FG, Groot H, Rauen U. Hypothermia causes a marked injury to rat proximal tubular cells that is aggravated by all currently used preservation solutions. Cryobiology. 2003; 47:82–91. [PubMed: 12963415]

40. Brinkkoetter PT, Song H, Losel R, Schnetzke U, Gottmann U, Feng YX, Hanusch C, Beck GC, Schnuelle P, Wehling M, van der Woude FJ, Yard BA. Hypothermic injury: the mitochondrial calcium, ATP and ROS love-hate triangle out of balance. Cellular Physiology and Biochemistry. 2008; 22:195–204. [PubMed: 18769046]

41. Maathuis MHJ, Leuvenink HGD, Ploeg RJ. Perspectives in organ preservation. Transplantation. 2007; 83:1289–1298. [PubMed: 17519776]

42. Sack MN. Mitochondrial depolarization and the role of uncoupling proteins in ischemia tolerance. Cardiovascular Research. 2006; 72:210–219. [PubMed: 16914124]

43. Honda HM, Korge P, Weiss JN. Mitochondria and ischemia/reperfusion injury. Communicative Cardiac Cell. 2005; 1047:248–258.

44. Piantadosi CA, Zhang J. Mitochondrial generation of reactive oxygen species after brain ischemia in the rat. Stroke. 1996; 27:327–331. [PubMed: 8571432]

45. Saba H, Munusamy S, MacMillan-Crow LA. Cold preservation mediated renal injury: involvement of mitochondrial oxidative stress. Ren Fail. 2008; 30:125–133. [PubMed: 18300110]

46. Murray J, Taylor SW, Zhang B, Ghosh SS, Capaldi RA. Oxidative damage to mitochondrial complex I due to peroxynitrite - Identification of reactive tyrosines by mass spectrometry. Journal of Biological Chemistry. 2003; 278:37223–37230. [PubMed: 12857734]

47. Radi R, Rodriguez M, Castro L, Telleri R. Inhibition of Mitochondrial Electron-Transport by Peroxynitrite. Archives of Biochemistry and Biophysics. 1994; 308:89–95. [PubMed: 8311480]

48. Davis CW, Hawkins BJ, Ramasamy S, Irrinki KM, Cameron BA, Islam K, Daswani VP, Doonan PJ, Manevich Y, Madesh M. Nitration of the mitochondrial complex I subunit NDUFB8 elicits RIP1-and RIP3-mediated necrosis. Free Radical Biology and Medicine. 2010; 48:306–317. [PubMed: 19897030]

49. Kanwar M, Chan PS, Kern TS, Kowluru RA. Oxidative damage in the retinal mitochondria of diabetic mice: possible protection by superoxide dismutase. Invest Ophthalmol Vis Sci. 2007; 48:3805–3811. [PubMed: 17652755]

50. Lee HB, Yu MR, Yang YQ, Jiang ZP, Ha H. Reactive oxygen species-regulated signaling pathways in diabetic nephropathy. Journal of the American Society of Nephrology. 2003; 14:S241–S245. [PubMed: 12874439]

51. Paradies G, Petrosillo G, Pistolese M, Ruggiero FM. Reactive oxygen species generated by the mitochondrial respiratory chain affect the complex III activity via cardiolipin peroxidation in beef-heart submitochondrial particles. Mitochondrion. 2001; 1:151–159. [PubMed: 16120275]

52. Han D, Williams E, Cadenas E. Mitochondrial respiratory chain-dependent generation of superoxide anion and its release into the intermembrane space. Biochemical Journal. 2001; 353:411–416. [PubMed: 11139407]

53. Muller FL, Liu YH, Van Remmen H. Complex III releases superoxide to both sides of the inner mitochondrial membrane. Journal of Biological Chemistry. 2004; 279:49064–49073. [PubMed: 15317809]

54. Ahlenstiel T, Burkhardt G, Kohler H, Kuhlmann MK. Improved cold preservation of kidney tubular cells by means of adding bioflavonoids to organ preservation solutions. Transplantation. 2006; 81:231–239. [PubMed: 16436967]

55. Bartels-Stringer M, Verpalen JT, Wetzels JF, Russel FG, Kramers C. Iron chelation or anti-oxidants prevent renal cell damage in the rewarming phase after normoxic, but not hypoxic cold incubation. Cryobiology. 2007; 54:258–264. [PubMed: 17391662]
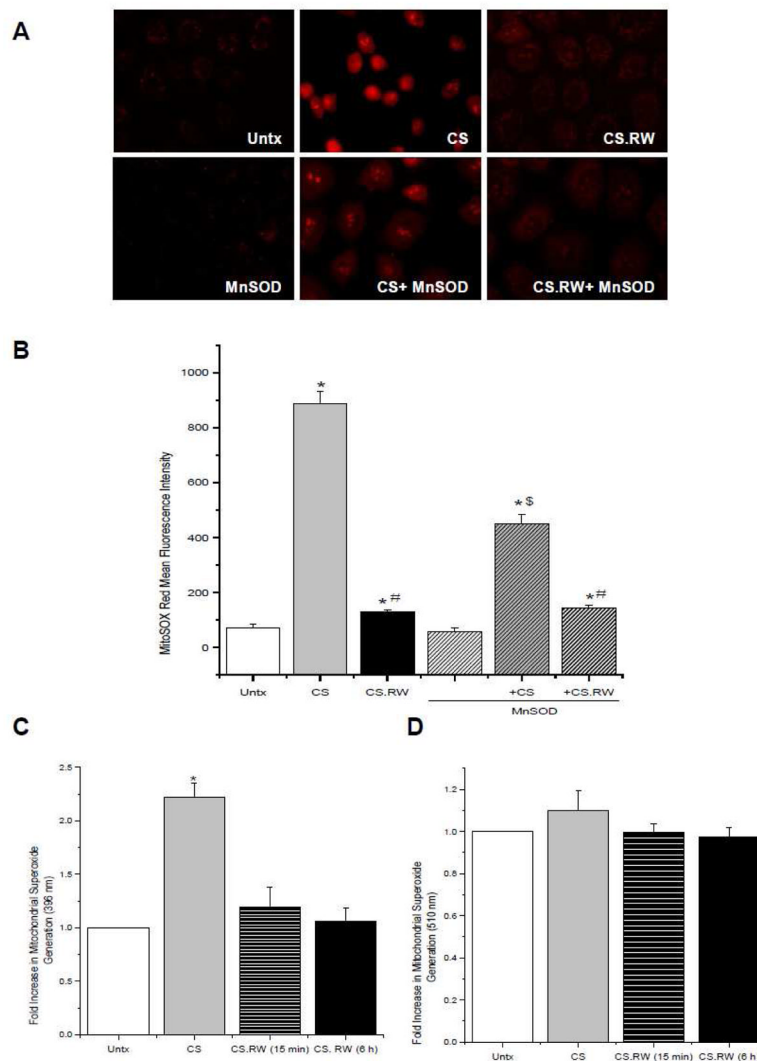
Figure 1.
Mitochondrial superoxide levels in NRK cells were evaluated using MitoSOX Red (5 μM for 10 min). **A**. Fluorescent microscopic images of (*left to right*): untreated (Untx) cells, cells exposed to CS, and cells exposed to CS followed by rewarming (CS.RW). Cells in the lower three images were treated similarly as the cells in the top panels, but were transiently transfected with MnSOD. Results are representative of 3 experiments using different cell cultures. **B.** MitoSOX Red staining was quantified using the Nis Elements software. Values are expressed as mean ± SEM (n = 3). * $P < 0.05$ compared to untreated cells (+/− MnSOD); [#] $P < 0.05$ compared to CS cells (+/− MnSOD); [$] $P < 0.05$ compared to CS cells (- MnSOD). **C.** Fluorescence spectrometry of NRK cells grown on coverslips and tested for fluorescence of mito-hydroxyethidium measured at excitation 396 nm/emission 580 nm and **D.** fluorescence of mito-ethidium measured at excitation 510 nm/emission 580 nm. Values are expressed as mean fold change in arbitrary fluorescence value over Untx cells ± SEM (n=3). * $P < 0.05$ compared to Untx cells.
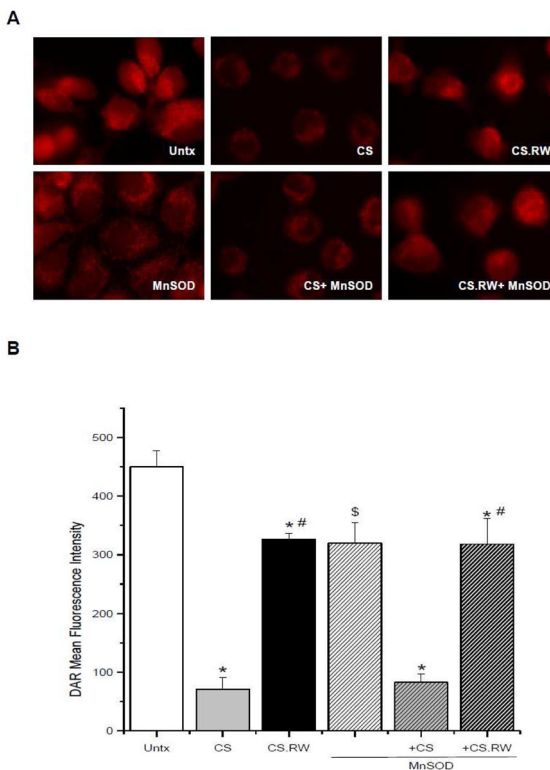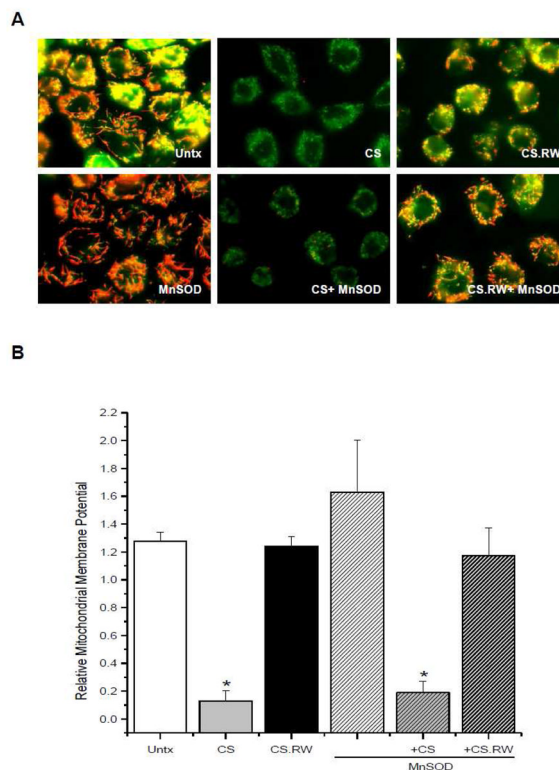
Figure 2.
Diaminorhodamine-4M AM (DAR; 5 µM for 30 min) was used to evaluate changes in available nitric oxide in cells exposed to CS or CS followed by RW (CS.RW). **A**. Fluorescent microscopic images of (*left to right*): untreated (Untx) cells, cells exposed to CS, and cells exposed to CS.RW. Cells in the lower three images were treated similarly as the cells in the top panels, but were transiently transfected with MnSOD. Results are representative of 3 experiments using different cell cultures. **B.** DAR fluorescence intensity was quantified using Nis Elements software. Values are expressed as mean ± SEM (n = 3). * $P < 0.05$ compared to untreated cells (+/− MnSOD); [#] $P < 0.05$ compared to cold stored cells; [$] $P < 0.05$ compared to untreated cells.
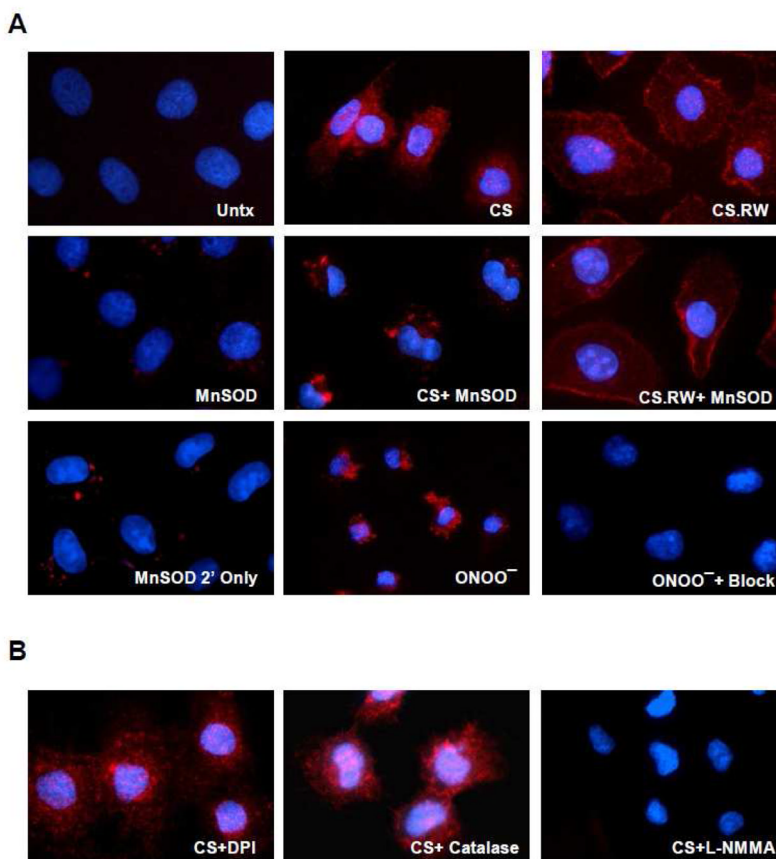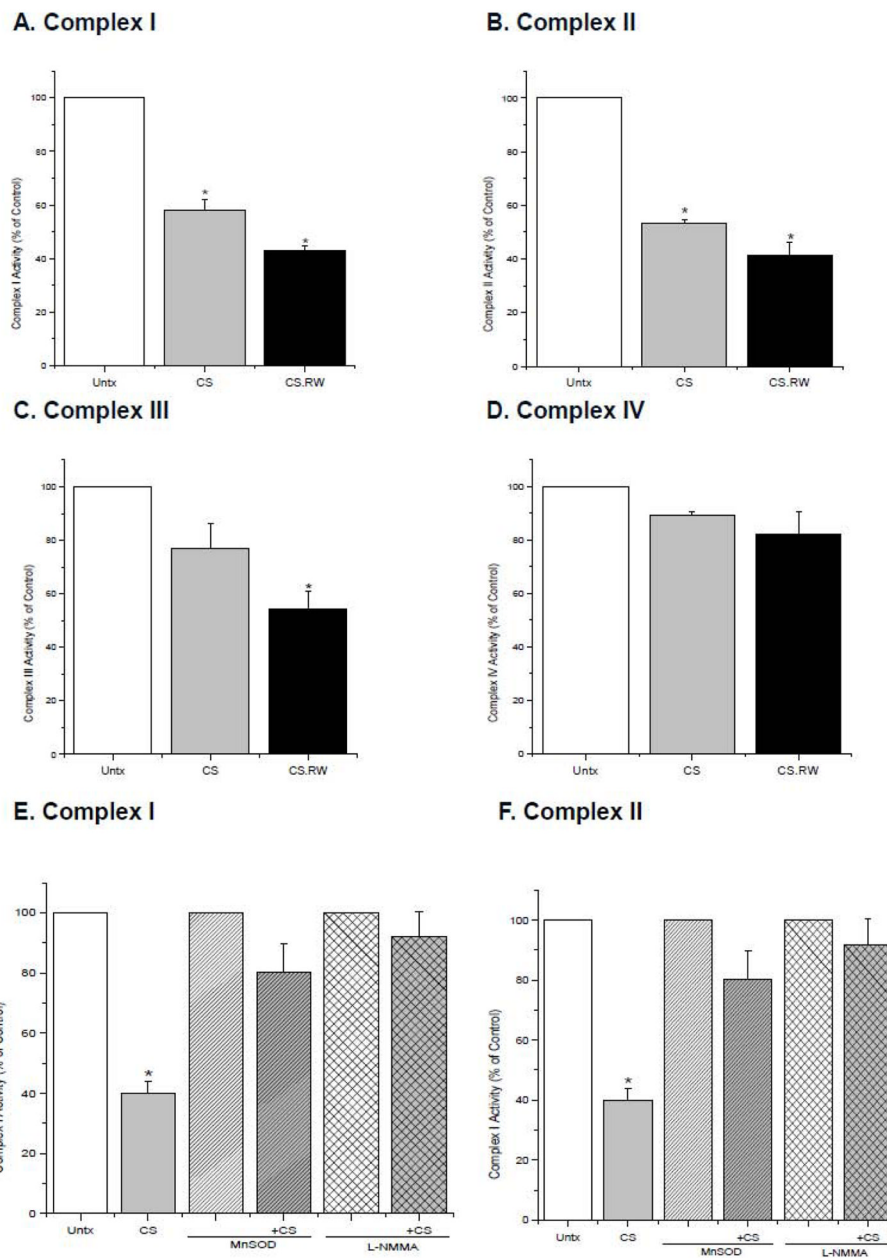
Figure 3.
Nitrotyrosine formation in NRK cells was assessed as described in the methods section. Briefly, NRK cells were incubated with a nitrotyrosine polyclonal antibody (1:200), followed by the secondary antibody conjugated with Alexa-594 (1:1000). Cells positive for nitrotyrosine fluoresce red and nuclear counterstaining (blue fluorescence) was evaluated using DAPI (1:100). **A**. Fluorescent microscopic images of (*left to right*): untreated (Untx) cells, cells exposed to CS, and cells exposed to CS followed by rewarming (CS.RW). Cells in the middle three images were treated similarly as the cells in the top panels, but were transiently transfected with MnSOD. The images depicted in the lower three panels represent staining controls: MnSOD overexpressing cells stained with secondary antibody alone, NRK cells treated with peroxynitrite (ONOO⁻) as a positive control, and NRK cells treated with ONOO⁻ but preincubated with excess 3-nitrotyrosine (negative control). **B**. Effect of oxidant inhibitors on nitrotyrosine formation was further evaluated. Fluorescent microscopic images of NRK cells exposed to 24 h of CS with three different drug pretreatments (*left to right*): DPI (NADPH oxidase inhibitor, 1μM for 1 h), Catalase (decomposes hydrogen peroxide, 2000 Units/mL for 30 min), and L-NMMA (NOS inhibitor, 100μM for 30 min). All drugs were incubated during CS as well. Results are representative of 3 experiments using different cell cultures.
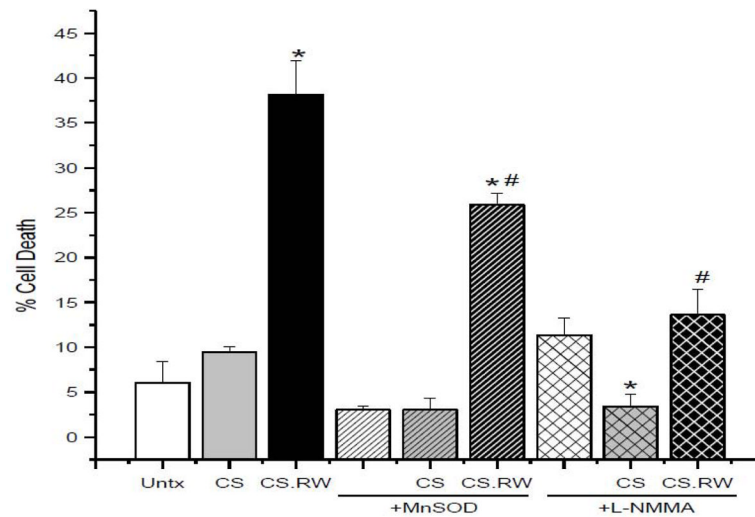
Figure 4.
JC-1 (7.5μM for 30 min) was used to measure the relative mitochondrial membrane potential of NRK cells. **A**. Fluorescent microscopic images of (*left to right*): untreated (Untx) cells, cells exposed to CS, and cells exposed to CS followed by rewarming (CS.RW). Cells in the lower three images were treated similarly as the cells in the top panels, but were transiently transfected with MnSOD. Results are representative of 3 experiments using different cell cultures. **B.** JC-1 fluorescence intensity was quantified using Nis Elements software. Relative mitochondrial membrane potential was calculated using the ratio of JC-1 aggregate/monomer (590 nm/530 nm) of mean fluorescence intensity. Values are expressed as mean ± SEM (n = 3). * P < 0.05 compared to untreated cells (+/− MnSOD).
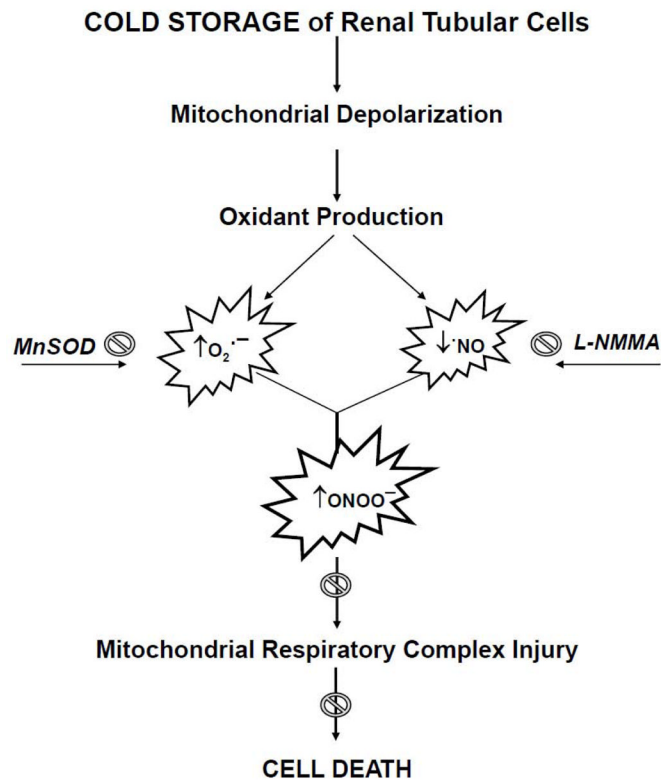
Figure 5.
Individual mitochondrial respiratory complex activities were measured using isolated mitochondria from NRK cells exposed to CS or CS followed by RW (CS.RW) (Graphs A–D). NRK cells were also transiently transfected with MnSOD or treated with L-NMMA (100 μM for 30 min prior to and during CS) (Graphs E–F). Values are expressed as percentage mean ± SEM (n = 3) of respective controls (set to 100). * P < 0.05 compared to respective controls.

Figure 6.
Cell death was assessed using the LDH Cytotoxicity Assay Kit II in NRK cells exposed to CS or CS followed by RW (CS.RW). NRK cells were also transiently transfected with MnSOD or treated with L-NMMA (100 μM for 30 min prior to and during CS.RW). Values are expressed as percentage cell death mean ± SEM (n = 3). * P < 0.05 compared to untreated cells in each respective group. # P < 0.05 compared to cells CS.RW in the untreated group.

Figure 7.
Schematic of hypothesized events occurring during cold storage (CS) and rewarming (RW) of NRK cells. CS induces mitochondrial membrane depolarization, increases mitochondrial superoxide ($O_2^{\bullet-}$) levels and decreases available nitric oxide ($^{\bullet}$NO) leading to peroxynitrite ($ONOO^-$) formation. Production of these mitochondrial oxidants contributes to mitochondrial respiratory complex inactivation and ultimately cell death. MnSOD overexpression (mitochondrial superoxide scavenger) and L-NMMA (nitric oxide inhibitor) treatment provides partial protection against mitochondrial and cellular injury of NRK cells during CS and RW.